phys. stat. sol. (a) **204**, No. 7, 2270–2278 (2007) / **DOI** 10.1002/pssa.200622498

Phase transition associated with the variation of oxygen vacancy/ion distribution in the oxide-ion conductor $La_2Mo_{2-x}W_xO_9$

D. Li[1], **X. P. Wang**[1, 2], **Q. F. Fang**[*, 1, 2], **J. X. Wang**[1], **C. Li**[1], and **Z. Zhuang**[1]

[1] Key Laboratory of Materials Physics, Institute of Solid State Physics, Chinese Academy of Sciences, Hefei 230031, P.R. China
[2] Ningbo Institute of Material Technology and Engineering, Chinese Academy of Sciences, Ningbo 315040, P.R. China

Received 16 October 2006, revised 30 January 2007, accepted 21 February 2007
Published online 24 April 2007

PACS 64.70.Kb, 66.30.Hs, 77.22.Gm, 81.05.Je

The effects of tungsten doping in $La_2Mo_{2-x}W_xO_9$ samples ($x = 0$, 0.1, 0.25, 0.5, 0.75, 1.0, 1.2, 1.4) were studied using dielectric relaxation measurements. Additional to the low-temperature relaxation peak P_d associated with oxygen ion diffusion, a new dielectric loss peak P_h was observed around 740 K. With increasing tungsten concentration, the activation energy of peak P_d increases and saturates at a value of about 1.45 eV, and the height of peak P_h increases at first and then decreases after passing a maximum at 25% tungsten doping. With increasing measurement frequency, the height of peak P_h decreases monotonically but its position shifts very little. Peak P_h in pure and tungsten-doped $La_2Mo_2O_9$ is suggested to be associated with a phase transition from the static disordered state to the dynamic disordered state of oxygen ion/vacancy distribution.

1 Introduction

Oxide-ion conductors have attracted considerable attention owing to their potential application in the fields of solid oxide fuel cells and other solid ionic devices [1–6]. Among these oxide-ion conductors, four distinct structural groups are well known: fluorite, perovskite, intergrowth perovskite/Bi_2O_3 layers and pyrochlore [3–8]. In 2000, Lacorre et al. [9, 10] reported a novel oxygen ionic conductor, $La_2Mo_2O_9$, with conductivity of about 0.06 S/cm at 800 °C, which is comparable to that of yttria-stabilized zirconia. In recent years $La_2Mo_2O_9$ has been extensively investigated owing to its excellent ionic conduction properties at intermediate temperatures (600–800 °C) and the new mechanism of oxygen vacancy formation based on the lone pair substitution concepts [9].

Analogous to other ionic conductors, this kind of material undergoes a structural transition around 580 °C from low-temperature monoclinic α-phase to high-temperature cubic β-phase, resulting in a decrease of conductivity by almost two orders of magnitude at lower temperatures. Most studies are focused on suppressing this phase transition and improving the degradation of hexavalent molybdenum under low oxygen pressure, which are two key factors that greatly limit the practical application of $La_2Mo_2O_9$. Doping or substituting at La and Mo sites with different cations has proved to be an effective method to solve these problems. Specially, it was found that the partial substitution of hexavalent tungsten for molybdenum could not only suppress the phase transition and increase the conductivity of

[*] Corresponding author: e-mail: qffang@issp.ac.cn, Phone: +86 551 5591459, Fax: +86 551 5591434

$La_2Mo_2O_9$, but also effectively enhance the electrochemical stability of $La_2Mo_2O_9$ [11–16]. This improvement of stability under reducing conditions is of great importance for the application of these kinds of materials as solid electrolytes.

In previous studies, a non-relaxational internal friction peak was observed in $La_2Mo_{2-x}W_xO_9$ [17], $La_{2-x}Ba_xMo_2O_{9-\delta}$ [18] and $La_{1.95}K_{0.05}Mo_{2-x}T_xO_{9-\delta}$ (T = Fe, Mn) [19], which was suggested to be associated with a phase transition from low-temperature static disordered state to high-temperature dynamic disordered state in distribution of oxygen ions/vacancies. In the work reported in this paper, to further understand the mechanism of this phase transition, a series of $La_2Mo_{2-x}W_xO_9$ samples (x = 0, 0.1, 0.25, 0.5, 0.75, 1.0, 1.2, 1.4) were prepared, and the effects of tungsten substitution for molybdenum on the oxygen ion diffusion and phase transition were systematically investigated using the dielectric relaxation (DR) method.

2 Experimental

Ceramic samples of $La_2Mo_{2-x}W_xO_9$ (x = 0, 0.1, 0.25, 0.5, 0.75, 1.0, 1.2, 1.4) were prepared by a conventional solid-state reaction method from a stoichiometric mixture of La_2O_3 (99.9%), MoO_3 (99.5%) and WO_3 (99%) powders. The well-mixed powders were calcined in an alumina crucible at 550 °C for 12 h in air, and then were ball milled and calcined at 1000–1150 °C several times depending upon the compositions. The obtained ceramic powders were finely ground and pressed into a mould to form pellets of size 8 mm diameter × 2 mm for the DR measurements. These pellets were finally sintered at 1050–1200 °C for 12 h in air depending upon the compositions, to ensure that the density of the ceramic samples reached as high as 94% of theoretical density.

The structural evolution of $La_2Mo_{2-x}W_xO_9$ materials with tungsten content was determined using X-ray diffraction (XRD). XRD patterns were recorded using a θ/θ Bragg–Brentano X'Pert MPD PRO diffractometer with $K\alpha_{1+2}$ radiations at room temperature. The program FullProf [20] refinement method was used to determine lattice parameters from the resultant spectra. Before DR measurements, silver films were deposited onto both sides of the samples as electrodes. The temperature spectra and frequency spectra of dielectric relaxation were measured using a Hioki 3531 Z Hi-tester instrument.

3 Results and discussion

3.1 Structure determination and crystal cell parameters

The room temperature XRD patterns for $La_2Mo_{2-x}W_xO_9$ with x = 0, 0.1, 0.5, 1.0, 1.4 are shown in Fig. 1. At first glance, all patterns are similar to that of β-phase (space group $P2_13$), and no other phases were found. Careful analysis reveals, however, that the unsubstituted specimen is α-phase, while the tungsten-substituted specimens with $x \geq 0.5$ exhibit β-phase. The difference between α- and β-phase is more visible on the diffraction patterns of the (123) reflection that splits due to the monoclinic distortion in α-phase, as enlarged in the right inset of Fig. 1. For the tungsten-substituted sample with x = 0.1, the width of the $K\alpha_1$ and $K\alpha_2$ components of the (123) reflection is wider than that in the samples with $x \geq 0.5$, implying that this level of tungsten substitution cannot completely suppress the α/β transition, namely the α- and β-polymorphs coexist in $La_2Mo_{1.9}W_{0.1}O_9$ specimens. This is discussed further in the following paragraphs.

The evolution of cell parameter with tungsten concentration was determined by refining the XRD patterns, as shown in the left inset of Fig. 1, where the lattice constant of α-phase is estimated by fitting the patterns with a pseudocubic phase. In the whole substitution level, a curved evolution of cell parameter with tungsten concentration is observed, i.e. the lattice constant increases first with the tungsten concentration, reaches a maximum of 0.7156 nm at x = 0.75, and then decreases. This evolution behavior is similar to that reported previously [12] where the increase of lattice constant at low doping content was interpreted in terms of the larger ionic radius of tungsten and the decrease of lattice constant at high doping content was explained in terms of the decrease in coordination number around tungsten.

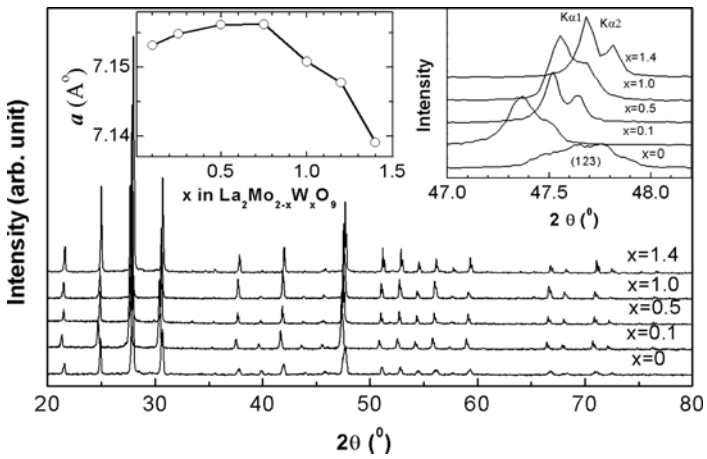

Fig. 1 XRD patterns of $La_2Mo_{2-x}W_xO_9$ ($x = 0$, 0.1, 0.5, 1.0, 1.4) at room temperature. The right inset shows the enlargement of the diffraction patterns of the (123) reflection and the left inset shows the evolution of cell parameters for $La_2Mo_{2-x}W_xO_9$.

3.2 Dielectric loss peaks in $La_2Mo_{2-x}W_xO_9$

The temperature dependence of dielectric loss (tan δ) of oxygen-ion conductor $La_2Mo_{2-x}W_xO_9$ ($x = 0$, 0.25, 0.5, 1.4) is presented in Fig. 2 for the temperature range 350–900 K. The results were obtained with a heating rate of 3 K/min at a frequency of 500 Hz. In all the investigated samples, two dielectric loss peaks, labeled as P_d and P_h, are observed. With increasing tungsten concentration, peak P_d obviously shifts towards higher temperature, from around 530 K for unsubstituted sample to 580 K for $La_2Mo_{0.6}W_{1.4}O_9$ sample, while for the peak P_h, located around 740 K, the peak position is almost independent of the ratio of W/Mo.

Except for peaks P_d and P_h, an obvious stepwise variation around 850 K is observed in the tan δ–T curves of the $La_2Mo_2O_9$ sample, as shown in Fig. 2. This stepwise variation of dielectric loss with temperature is actually associated with the α/β phase transition in $La_2Mo_2O_9$, as evidenced by an internal friction peak around this temperature in our previous work [21]. When the tungsten doping concentration

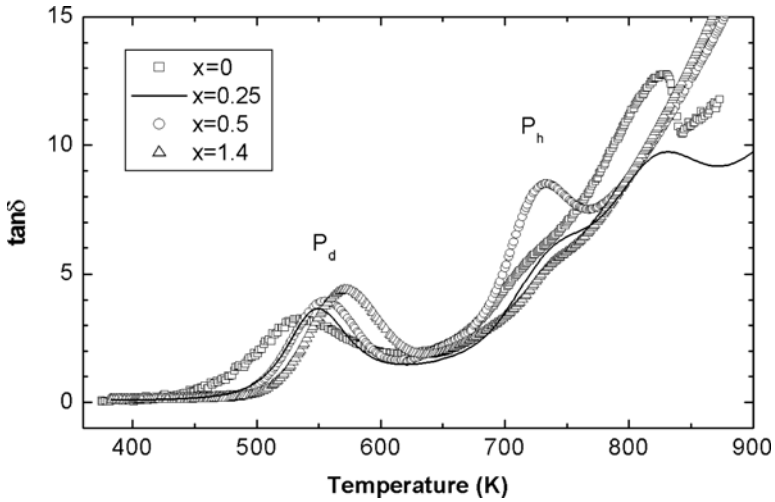

Fig. 2 Variation of dielectric loss versus temperature for $La_2Mo_{2-x}W_xO_9$ ($x = 0$, 0.25, 0.5, 1.4) at a frequency of 500 Hz.

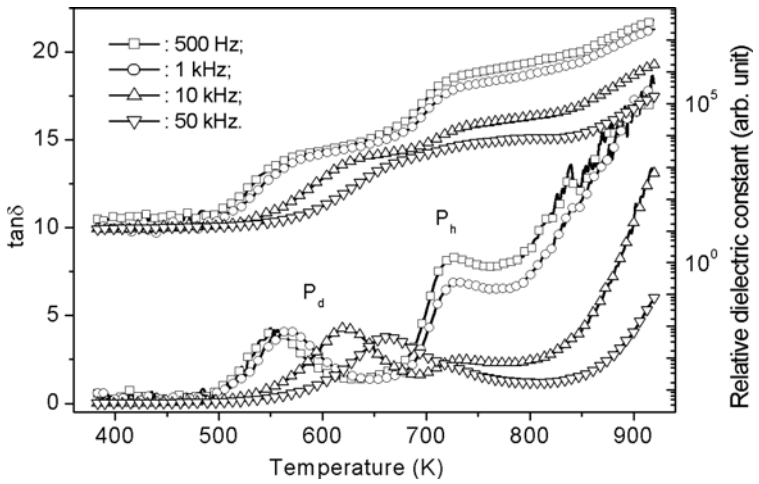

Fig. 3 Variation of dielectric loss and relative dielectric constant with temperature for $La_2Mo_{1.5}W_{0.5}O_9$ sample at four different frequencies, as indicated.

reaches 12.5%, the stepwise variation still occurs but becomes a little smaller, indicating that the β-phase cannot be completely stabilized to lower temperature for this doping concentration. With the tungsten doping content further increasing to 25%, the dielectric loss curve changes smoothly in the region of the phase transition temperature. These results indicate that for a tungsten substitution level $x \geq 0.5$, the α/β transition can be completely suppressed, and the high-temperature phase is stabilized to lower temperature, in agreement with results reported previously [15, 16].

To further understand the features of peaks P_d and P_h, more careful experiments were carried out at different frequencies. As an example, Fig. 3 illustrates the variation of dielectric loss and relative dielectric constant with temperature for a $La_2Mo_{1.5}W_{0.5}O_9$ sample at four different frequencies. It is obvious that with increasing frequency peak P_d shifts towards higher temperature, while peak P_h hardly changes its position. Moreover, the height of peak P_h decreases rapidly with increasing frequency, but peak P_d is almost constant in height. Correspondingly, the relative dielectric constant changes dramatically in the temperature range around the peak positions. From the behaviors of these two peaks with frequency, one can say that peak P_d corresponds to a relaxational process while peak P_h seems to be associated with a phase transition process.

3.3 Activation energy measurement and mechanism of peak P_d

For a relaxational peak one has the following relations at the peak position:

$$\omega\tau = 1 \tag{1}$$

and

$$\tau = \tau_0 \exp(E/kT)\,, \tag{2}$$

where ω is the measurement circular frequency, k is the Boltzmann constant, τ and τ_0 are the relaxation time at temperature T and at infinite temperature, respectively, and E is the activation energy of the corresponding relaxation process. Therefore, if one plots the so-called Arrhenius relation (i.e. ln ω_p versus $1/T_p$, where subscript 'p' means the value at peak position, as shown in the inset of Fig. 4 as an example for a La_2MoWO_9 sample), the values of E and τ_0 can be deduced as 1.15–1.45 eV and 10^{-13}–10^{-16} s, respectively. The activation energy of peak P_d increases dramatically from about 1.15 eV for the unsubstituted sample to 1.31 eV for the lowest substituted member ($x = 0.1$), as shown in Fig. 4. On further increasing the tungsten concentration, the activation energy slowly increases and then saturates at a value

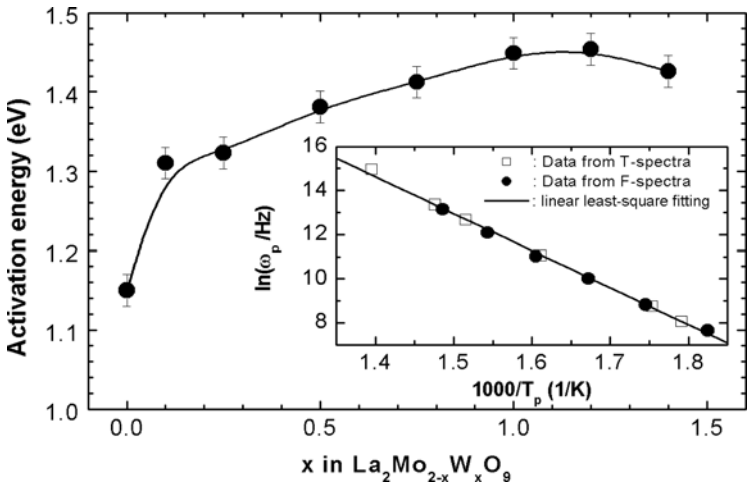

Fig. 4 Variation of the activation energy of peak P_d with tungsten concentration. The inset shows the Arrhenius plot of peak P_d in a La_2MoWO_9 sample. The open and filled squares are from the temperature spectra and the frequency spectra, respectively. The line is the result of least-squares fitting. The logarithmic scale of the inset is the natural logarithm.

of about 1.45 eV. The initial increase of activation energy reflects the blocking effect of tungsten substitution on oxygen ion diffusion due to the large ionic radius of tungsten.

In our previous studies [22–24], peak P_d was detected in the dielectric spectrum in $La_2Mo_2O_9$ as well as other substituted compounds, where the mechanism of peak P_d was interpreted as the short-distance diffusion of oxygen ions via vacancies. In solid-state oxide ceramics, the oxygen vacancy not only forms an elastic dipole but also an electric dipole, if the site at which the oxygen vacancy locates has a lower symmetry than the lattice. In $La_2Mo_2O_9$, since the sites of O(2) and O(3) have lower symmetry, the vacancies at such sites are localized and immobile at lower temperature and form electric dipoles [22]. In the action of an alternating electric field the electric dipoles result in the process of dipolar relaxation [25]. The values of the relaxation parameters of peak P_d are in the same range as that for oxygen ion diffusion in oxide ceramics [26], confirming the mechanism of short-distance diffusion of oxygen ions via vacancies for peak P_d. However, the activation energy of relaxation peak P_d is a little lower than that of the conductive activation energy [27]. This is reasonable because the conductive activation energy is measured at higher temperature and related to the long-distance diffusion of oxygen ions, while the relaxation activation energy is measured at lower temperature and related to the short-distance jumps of oxygen ions.

3.4 Possible mechanism of peak P_h in $La_2Mo_{2-x}W_xO_9$

Figure 5 shows the variation of dielectric loss with frequency for a $La_2Mo_{1.5}W_{0.5}O_9$ sample at three temperatures. Peak P_d appears around 500 kHz and it shifts to higher frequency with increasing temperature. The values of E and τ_0 can be determined as 1.34 eV and 2.8×10^{-16} s, which correspond to the E and τ_0 of peak P_d in the temperature spectra, further reinforcing the relaxational argument. The absence of peak P_h in the frequency spectra illustrates from another side that peak P_h is non-relaxational because for a non-relaxational peak in the temperature spectra there is no correspondence in the frequency spectra.

The non-relaxational nature of peak P_h can be further verified by the following data analysis. Using a nonlinear fitting method [28], the temperature spectra of DR in all $La_2Mo_{2-x}W_xO_9$ samples can be fitted by an exponential background and two Debye functions in the form:

$$\tan\delta = \Delta\frac{\omega\tau}{1+\omega^2\tau^2} \tag{3}$$

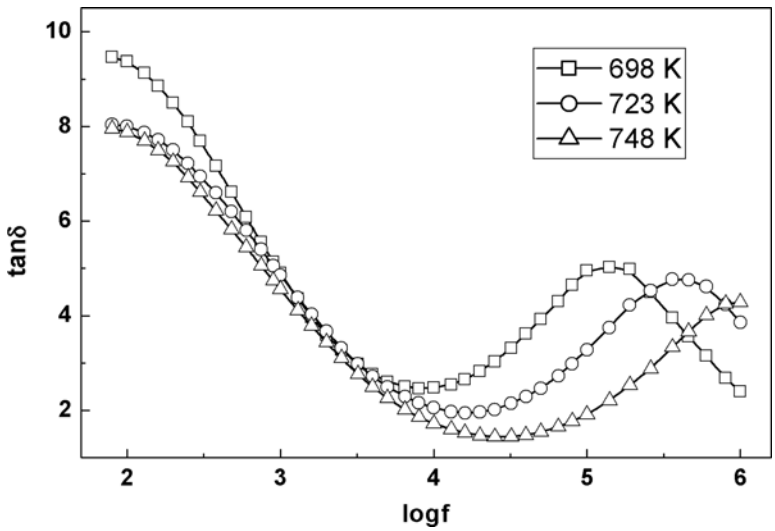

Fig. 5 Variation of dielectric loss with frequency for a $La_2Mo_{1.5}W_{0.5}O_9$ sample at the three temperatures indicated. The frequency scale is the logarithm to the base 10.

where A is a constant. The fitting results are satisfactory in the aspect that the total fitting lines pass through almost all data points, as shown in Fig. 6 as an example for a $La_2Mo_{1.5}W_{0.5}O_9$ sample at 500 Hz. It is abnormal that peak P_h can be well fitted by a Debye function, because the Debye function is usually used to describe the peak shape of a relaxational peak. From another side, careful analysis indicates that the position of peak P_h shifts a little towards higher temperature with increasing frequency, as shown in the inset of Fig. 6 for a $La_2Mo_{1.5}W_{0.5}O_9$ sample. Do these facts suggest that peak P_h possess some relaxational nature? The answer is negative because the shift of P_h with frequency is so small that if we estimate activation energy by using the Arrhenius relation, a value of 9 eV is obtained. Such high activation energy at 740 K has no physical meaning but indicates the non-relaxational nature of peak P_h.

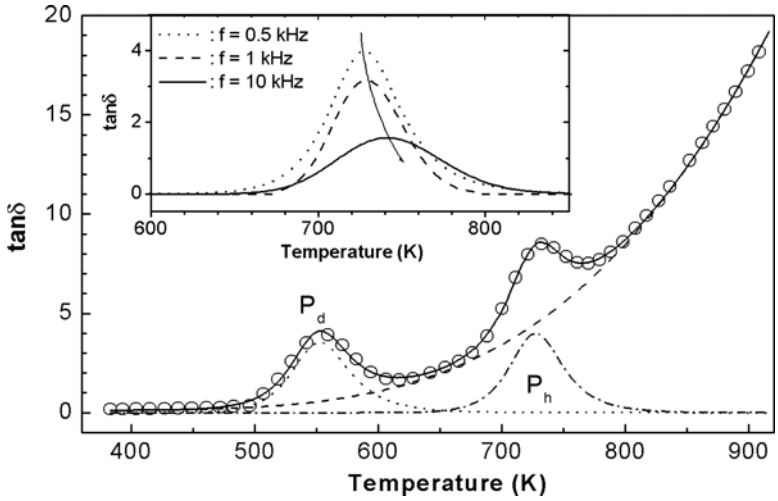

Fig. 6 Fitting results of the dielectric loss curve at 500 Hz for a $La_2Mo_{1.5}W_{0.5}O_9$ sample. The symbols are the experimental data points and the solid line is the total fitting curve. The dashed, dotted and dash-dotted lines are fitted background, P_d peak and P_h peak, respectively. The inset shows the fitting results of the P_h peaks at the three frequencies indicated.

The non-relaxational feature of peak P_h prompt us to conclude that peak P_h is associated with a process of phase transition, although its peak shape coincides with a Debye function and its position changes a little with frequency. Moreover, this phase transition is a new process and quite different from the first-order α/β phase transition, because these two transition processes coexist in samples of pure and low-content tungsten-doped $La_2Mo_2O_9$ and locate as far as 100 K. Indeed, differential thermal analysis (DTA) measurement and variable-temperature XRD patterns have not shown any trace of phase transition around the peak temperature of P_h (but for the α/β phase transition it does), indicating that this phase transition if it ever occurs, is neither symmetry breaking nor endothermic/exothermic.

In the oxygen sublattice of cubic LAMOX compounds, the high atomic displacement parameters deduced from XRD and neutron diffraction measurements suggest that the oxygen ions are delocalized, especially at the oxygen sites of O(2) and O(3) [29–32]. The extent of delocalization will obviously increase with increasing temperature, and at a given temperature where the zones of delocalization of two neighboring oxygen ions overlap with each other a random distribution of oxygen ions is formed. This is the so-called dynamic disordered state in the oxygen sublattice where the oxygen ions and the vacancies can exchange their position easily and rapidly owing to the thermally assisting mechanism as suggested in Ref. [33]. With decreasing temperature, the dynamic disordered state will be frozen and changes to a static disordered state in cubic LAMOX compounds where the thermally assisted exchanging rate between oxygen ions and vacancies is much smaller. Therefore at a given temperature the phase transition from the static disordered state to the dynamic disordered state of oxygen ion/vacancy distribution occurrs, which is similar to the glass transition process in amorphous compounds and polymers as well as to the formation process of spin glass in ferromagnetic materials. Since this phase transition occurred in the oxygen sublattice, it will not break the symmetry and therefore cannot be detected by DTA and thermal XRD, but will be reflected by an internal friction peak in tungsten- and barium-substituted $La_2Mo_2O_9$ [17, 18], by the present dielectric loss peak P_h, and by the transition of conduction mechanism from the Arrhenius type at low temperature to the VTF (Vogel–Tamman–Fulcher) type at high temperature [32].

This kind of phase transition would depend strongly not only on the oxygen sublattice but also on the cationic sublattice. The introduction of W^{6+} at Mo site in $La_2Mo_2O_9$ would result in distortion of the lattice and the distribution of this distortion would be non-homogeneous in nature. Therefore, the phase transition would occur at different temperatures at different zones in the lattice. This effect will widen the temperature range of the transition process and broaden the dielectric loss peak corresponding to this phase transition, which is similar to the disperse phase transition in ferroelectric materials. This may be the reason why peak P_h has a form similar to a Debye function.

It is noted, however, that the dielectric loss peak P_h is located around 740 K, much higher than the value of 640 K of the internal friction peak. This discrepancy in peak position (or the temperature of phase transition) may be understood from the following two aspects. One aspect is the higher frequency used in dielectric loss measurement than in the internal friction measurement. The so-called 'freezing' of the dynamic disordered state means that the exchange rate between oxygen ions and vacancies is much lower than the externally applied detecting frequency (here it is the frequency used in the dielectric loss and internal friction measurement). Dielectric loss measurement with higher frequency will detect a higher freezing temperature, which is also one of the possible reasons why peak P_h shifts a little towards higher temperature with increasing frequency. The other aspect is that oxygen vacancies or ions respond to the externally applied alternative electric field (for dielectric loss) and stress field (for internal friction) differently.

Figure 7 shows the height and position of peak P_h as a function of tungsten concentration x in $La_2Mo_{2-x}\cdot W_xO_9$. The peak temperature of peak P_h increases from about 720 K in pure $La_2Mo_2O_9$ to 750 K in 5% tungsten-doped sample, then decreases and saturates around 730 K. With increasing tungsten doping, the peak height of peak P_h increases at first, and then decreases after passing a maximum at a tungsten doping content of 25% where the α/β phase transition is completely suppressed. The fact that peak P_h with low intensity appears in pure α-$La_2Mo_2O_9$ illustrates the existence of small amounts of disordered states in pure α-$La_2Mo_2O_9$, as pointed out previously [34], which also undergoes the transition from the dynamic disordered state to the static disordered state.

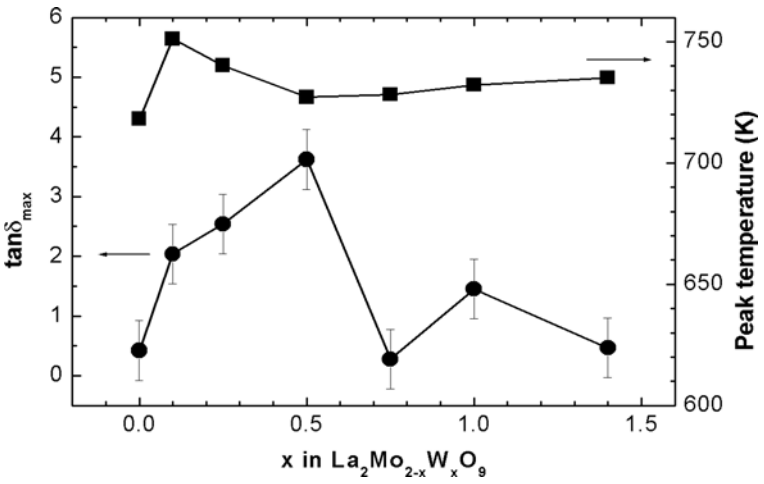

Fig. 7 Height and position of peak P_h as a function of doped tungsten concentration x in $La_2Mo_{2-x}W_xO_9$.

4 Conclusions

The main results in this paper can be summarized as follows:

1. Two dielectric loss peaks (P_d at lower temperature and P_h at higher temperature) were observed in pure and tungsten-substituted $La_2Mo_2O_9$ samples.

2. Peak P_d is of relaxation type and is related to the short-distance jumps of oxygen vacancies. The activation energy of peak P_d at first increases and then saturates at a value of about 1.45 eV with increasing tungsten concentration, which indicates that partial substitution of W^{6+} ions at Mo^{6+} sites will increase the difficulty of oxygen-ion diffusion in crystal lattices.

3. With increasing tungsten concentration, the height of peak P_h increases at first and then decreases after passing a maximum at 25% tungsten doping. With increasing measurement frequency, the height of peak P_h decreases monotonically but its position shifts very little. Peak P_h is suggested to be associated with a phase transition from the static disordered state to the dynamic disordered state of oxygen ion/vacancy distribution.

4. In pure $La_2Mo_2O_9$, the appearance of small peak P_h indicates the existence of small amounts of disordered states in pure α-$La_2Mo_2O_9$ that also undergo the transition from the dynamic disordered state to the static disordered state.

Acknowledgements This work was subsidized by the National Natural Science Foundation of China (Grant No. 50672100), by the Ningbo Civic Natural Science Foundation, China (Grant No. 2006A610057) and by the Anhui Provincial Natural Science Foundation, China (Grant No. 0504440901).

References

[1] H. Yahiro, T. Ohuchi, and K. Eguchi, J. Mater. Sci. **23**, 1036 (1988).
[2] A. Pimenov, J. Ullrich, P. Lunkenheimer, A. Loial, and C. H. Rscher, Solid State Ion. **109**, 111 (1988).
[3] N. Q. Minh, J. Am. Ceram. Soc. **76**, 563 (1993).
[4] K. R. Kendall, C. Navas, J. K. Thomas, and H. C. Z. Loye, Solid State Ion. **82**, 215 (1995).
[5] J. A. Lane, S. J. Benson, D. Waller, and J. A. Kilner, Solid State Ion. **121**, 201 (1999).
[6] J. A. Kilner, Solid State Ion. **13**, 129 (2000).
[7] T. Ishihara, H. Matsuda, and Y. Yakita, J. Am. Chem. Soc. **116**, 3081 (1994).
[8] A. S. Kramer and H. L. Tuller, Solid State Ion. **82**, 15 (1995).
[9] P. Lacorre, Solid State Sci. **2**, 755 (2000).
[10] P. Lacorre, F. Goutenoire, O. Bohnke, and R. Retoux, Nature **404**, 856 (2000).

[11] S. Georges, F. Goutenoire, Y. Laligant, and P. Lacorre, J. Mater. Chem. **13**, 2317 (2003).
[12] G. Corbel, Y. Laligant, F. Goutenoire, E. Suard, and P. Lacorre, Chem. Mater. **17**, 4678 (2005).
[13] J. H. Yang, Z. H. Gu, Z. Y. Wen, and D. S. Yan, Solid State Ion. **176**, 523 (2005).
[14] S. Georges, F. Goutenoire, P. Lacorre, and M. C. Steil, J. Eur. Ceram. Soc. **25**, 3619 (2005).
[15] D. Marrero-Lopez, J. Canales-Vazquez, J. C. Ruiz-Morales, J. T. S. Irvine, and R. Nunez, Electrochim. Acta **50**, 4385 (2005).
[16] D. Marrero-Lopez, J. Canales-Vazquez, W. Z. Zhou, J. T. S. Irvine, and P. Nunez, J. Solid State Chem. **179**, 278 (2006).
[17] X. P. Wang, D. Li, Q. F. Fang, Z. J. Cheng, G. Corbel, and P. Lacorre, Appl. Phys. Lett. **89**, 021904 (2006).
[18] F. J. Liang, X. P. Wang, Q. F. Fang, J. X. Wang, C. Li, D. Li, and Z. Zhuang, Phys. Rev. B **74**, 014112 (2006).
[19] C. Li, X. P. Wang, J. X. Wang, D. Li, Z. Zhuang, and Q. F. Fang, J. Appl. Phys. (in press).
[20] J. Rodriguez-Carvajal, FullProf 2K program, version 2.00, Nov. 2001.
[21] X. P. Wang and Q. F. Fang, J. Phys.: Condens. Matter **13**, 1641 (2001).
[22] X. P. Wang and Q. F. Fang, Phys. Rev. B **65**, 064304 (2002).
[23] X. P. Wang, Z. J. Cheng, and Q. F. Fang, Solid State Ion. **176**, 761 (2005).
[24] X. P. Wang, Q. F. Fang, Z. S. Li, G. G. Zhang, and Z. G. Yi, Appl. Phys. Lett. **81**, 3434 (2002).
[25] C. Ang and Z. Yu, Phys. Rev. B **62**, 228 (2000).
[26] M. Weller and H. Schubert, J. Am. Ceram. Soc. **69**, 573 (1986).
[27] S. Georges, O. Bohnke, F. Goutenoire, Y. Laligant, J. Fouletier, and P. Lacorre, Solid State Ion. **177**, 1715 (2006).
[28] Q. F. Fang, X. P. Wang, G. G. Zhang, and Z. J. Cheng, phys. stat. sol. (a) **202**, 1041 (2005).
[29] F. Goutenoire, O. Isnard, and P. Lacorre, Chem. Mater. **12**, 2575 (2000).
[30] S. Georges, F. Goutenoire, F. Altorfer, D. Sheptyakov, F. Fauth, E. Suardkinner, and P. Lacorre, Solid State Ion. **161**, 231 (2003).
[31] I. R. Evans, J. A. K. Howard, and J. S. O. Evans, Chem. Mater. **17**, 4074 (2005).
[32] S. Georges, F. Goutenoire, O. Bohnke, M. C. Steil, S. J. Skinner, H.-D. Wiemhöfer, and P. Lacorre, J. New Mater. Electrochem. Syst. **7**, 51 (2004).
[33] O. Bohnke, C. Bohnke, and J. L. Foruquet, Solid State Ion. **91**, 21 (1996).
[34] J. Emery, D. Massiot, P. Lacorre, Y. Laligant, and K. Conder, Magn. Reson. Chem. **43**, 366 (2005).

